CHEMICAL COMPONENT YIELD 2022

by Anton Irawan

Submission date: 05-Apr-2023 03:59PM (UTC+0700)
Submission ID: 2056460810
File name: 2022_Chemical_Component_Yield.pdf (4.69M)
Word count: 9848
Character count: 50106

Journal of Analytical and Applied Pyrolysis 161 (2022) 105399

Contents lists available at ScienceDirect

Journal of Analytical and Applied Pyrolysis

journal homepage: www.elsevier.com/locate/jaap

Chemicals component yield prediction and kinetic parameters determination of oil palm shell pyrolysis through volatile state approach and experimental study

Pandit Hernowo [a,b], Soen Steven [a], Elvi Restiawaty [a,c], Anton Irawan [d], Carolus Borromeus Rasrendra [a,c], Septhian Marno [e], Yana Meliana [e], Yazid Bindar [a,c,*]

[a] Department of Chemical Engineering, Faculty of Industrial Technology, Institut Teknologi Bandung, Bandung 40132, Indonesia
[b] Department of Chemical Engineering, Institut Sains dan Teknologi Al-Kamal, Jakarta Barat 11520, Indonesia
[c] Department of Bioenergy Engineering and Chemurgy, Faculty of Industrial Technology, Institut Teknologi Bandung, Bandung 40132, Indonesia
[d] Department of Chemical Engineering, Faculty of Engineering, University of Sultan Ageng Tirtayasa, Banten 42435, Indonesia
[e] Research and Technology Center Pertamina, PT. Pertamina, Pulo Gadung, Jakarta Timur, Indonesia

ARTICLE INFO

Keywords:
Green chemicals
Fuels
Arrhenius constant
Benzene
Toluene
Xylene

ABSTRACT

The green products from biomass pyrolysis open the way for the development and application of alternative fuels and chemicals. Until now, the pyrolysis kinetic studies are derived from solid-state approach (based on biomass as a reactant) which still faced drawbacks. A new approach, namely volatile state approach, is then develop with the volatile products as the main basis or reference to predict the mass fraction and yield as well as to determine the kinetic parameters from oil palm shell pyrolysis. The predicted results were then validated with the semi-batch pyrolysis experimental st The oil palm shell has a biomass type number (N_{CT}) of 9.57, volatile matter (Y_{VM}) of 71.90%-wt, and was pyrolyzed at 300 °C, 350 °C, 400 °C, 450 °C, and 500 °C. From the experiment, as many as 95 compounds in bio-crude oil (BCO) were successfully produced which contain 72.79%-wt water and 27.21%-wt organic compounds. According to the characterization of 15 BCO components, they were classified into carbohydrates, fatty acids, phenol, aromatics, and water. Furthermore, the activation energy of products formation revealed a temperature dependence as a second-order polynomial function. Ultimately, this approach shows its satisfying capability to predict each BCO component mass fraction and yield which closely fits the experimental results.

1. Introduction

Nowadays, the use of fossil fuels for energy and chemicals purposes must be abandoned because of threatening the environment and humans [1–4]. Therefore, another resource to support energy security should be employed. Th lignocellulosic biomass resources from agricultur-e/plantations play an important role to replace fossil fuels with green chemicals as well as alternative energy development [5,6]. One of the Indonesian potential biomass is oil palm shell which was widely generated in oil palm processing [7]. Oil palm shell has a high volatile matter (62–85%) as well as high oil yield (up to 35.9%) compared to other biomass [8] which becomes pro ising to be utilized for producing green chemicals. The utilization is through pyrolysis as one of the biomass thermal conversion with the suppressed amount of oxygen to obtain char and volatile which consists of bio-crude oil (BCO) and bio-pyrolysis gas (BPG) [5,9]. The BCO usually contains oxygenate compounds [10,11] and BPG consists of light gas mixtures [12].

Up to now, biomass pyrolysis kinetic studies still refer to reactant, known as solid-state approach [13]. This approach scrutinized the biomass decomposition behavior in thermal gravimetric analysis (TGA) instrument which on easured mass loss [13–15]. There are also de-velopments such as one-step global kinetic, one-stage multi-reaction kinetic, and two-stage semi-global kinetic [16]. Unfortunately, those are still not able to determine the volatile mass fraction and yield. Likewise, it should be notified that biomass amount is always declining at any time and temperature. This leads to inconsistent kine law equations and varying values of kinetic parameters, which are the main weakness of solid-state approach [17].

* Corresponding author at: Department of Chemical Engineering, Faculty of Industrial Technology, Institut Teknologi Bandung, Bandung 40132, Indonesia.
E-mail address: ybybyb@fti.itb.ac.id (Y. Bindar).

https://doi.org/10.1016/j.jaap.2021.105399
Received 14 September 2021; Received in revised form 10 November 2021; Accepted 26 November 2021
Available online 30 November 2021

The researches conducted by Di Blasi and Branca (2001), as well as Grønli et al. (2002), have attempted to predict the volatile mass fraction and yield [18,19]. Furthermore, the studies from the research group led by Di Blasi have mostly focused on characterizing the volatile products from pyrolysis of wood and other agricultural biomass. Nevertheless, the studies of determining mass fraction, yield, and kinetic parameters based on the volatile components using volatile state approach still have not been carried out [20–22]. Actually, the volatile can be presumed to consist of BCO, CH_4, CO, CO_2, H_2O, H_2, and C_xH_y as a hard-identified light gas component, but the calculation certainly must comply with the law of mass conservation [23].

Meanwhile, Ranzi et al. (2008) delivered a kinetic model of volatile products formation for complex multi-step observations. The biomass was assumed to be cellulose, hemicellulose, and lignin in a separated form, so the model is also known as lumped kinetic scheme [24]. The results indicate that biomass primary decomposition can be modeled by considering the thermal behavior of cellulose, hemicellulose, and lignin [25,26]. Hemicellulose decomposes at 498–598 K, cellulose at 598–648 K, and lignin decomposes gradually in the temperature range of 523–773 K [27]. Yet, the lumped kinetic scheme is complex and still discusses the biomass thermal degradation behavior from the separated components and not from the direct lignocellulosic as a whole [28].

Another development of pyrolysis kinetic model employed the Gaussian distribution, which presumes pyrolysis is a first-order reaction with the parallel-independent rate having a continuously distributed activation energy [29–31]. Unfortunately, it has high complexity [32] and also has weakness in its curve symmetry where volatile production forms an asymmetric sigmoidal curve [33]. In addition, the kinetic scheme of biomass pyrolysis is realized to be highly complex [34]. Thus, it is recommended to be modeled with first-order pseudo kinetic which gives more suitable results of volatile products formation [35,36]. This is evidenced and strengthened by the identical range of Arrhenius factor value as well as relatively close activation energy value in the temperature range of 400–460 °C [36].

From the previous exposition, the still-not-success in predicting the volatile mass fraction and yield makes it urgent to develop a new approach, named as volatile state approach, which also applies the first-order pseudo kinetic concept. The volatile matter release from pyrolysis and its relationship with biomass characteristics in the form of proximate analysis leads to the beginning of the volatile state approach development [29,37]. Interestingly, this approach has the ability to predict the activation energy value of each volatile component which still follows mass conservation [38]. The development began from the pyrolysis study on 25 types of biomass which resulted in a ratio of actual volatile yield (Y_{VY}) to volatile matter (Y_{VM}) greater than one, which implied that obtained volatile amount could exceed the value from the proximate analysis [29]. Additionally, the pyrolysis study of fine coal particles performed by Mill (2000) has succeeded to prove that volatile release could exceed the volatile matter which was measured in the proximate condition. The ratio of these two parameters is then called volatile enhancement, V_E [37].

In addition, Bindar [38] describes that V_E is a polynomial function, $f_5\left(\frac{T}{T_s}\right)$, and aims to correct the proximate process condition to the actual pyrolysis process condition [38]. The volatile state approach has initially been applied by Hernowo et al. [17] to predict the yield and mass fraction of chemicals component produced from biomass pyrolysis [17]. The results showed that the developed approach is able to determine the component mass fraction and yield with an excellent agreement to the experimental data from Nunn et al. [39] as well as Branca et al. [40]. However, it is important to validate this approach under experiment using different biomass types, pyrolysis conditions, and also pyrolysis apparatus.

This study, hence, intends to predict the mass fraction and yield of volatile products as well as determine the kinetic parameters using volatile state approach from oil palm shell pyrolysis. All of the predicted results were then validated by pyrolysis experiment in semi-batch mode. Due to the exposure to high heat in the pyrolysis, biomass was decomposed and then continued with volatile matter quenching by water at room temperature [5]. The condensed volatile matter (BCO) was collected in the product tank and its chemical composition was then identified and measured.

Table 1
The differential and integral forms of first-order mechanism using solid-state and volatile state approaches.

	Differential Form	Integral Form
Solid-state	$1-\alpha$	$-ln(1-\alpha)$
Volatile state	$1-Y_{VY,P} = 1-e^{f_5\left(\frac{T}{T_s}\right)+f_2(N_{CT})}$	$-ln\left(1-Y_{VY,P}\right) = -ln\left(1-e^{f_5\left(\frac{T}{T_s}\right)+f_2(N_{CT})}\right)$

2. Prediction model and experimental section

2.1. Volatile state approach calculations

The calculations start from oil palm shell physicochemical properties and chemical composition [38,41]. Basically, the chemical composition is represented by ultimate analysis while the information about moisture, volatile matter, fixed carbon, and ash are embedded in proximate analysis. The ultimate analysis is strongly related to biomass type number (N_{CT}), as stated in Eq. 1. Afterward, the relationship between the predicted volatile matter amount ($Y_{VM,p}$) and N_{CT} is written in Eqs. 2 and 3 [38].

$$N_{CT} = \frac{Y_C}{Y_H}.\frac{Y_C}{Y_O} \tag{1}$$

$$Y_{VM,p} = e^{f_2(N_{CT})} \times 100\% \tag{2}$$

$$f_2(N_{CT}) = 0.031 - 0.029\,ln(N_{CT}) - 0.038(ln\,N_{CT})^2 \tag{3}$$

Different biomass types lead to the unique value of predicted volatile yield ($Y_{VY,p}$) which is acquired following Eq. 4. The function $f_5\left(\frac{T}{T_s}\right)$ is specified using Eq. 5 by inserting T_s as the standard temperature for proximate analysis, 900 °C [38]. In accordance with Xu and Tomita (1987), the actual volatile yield (Y_{VY}) composed of bio-crude oil (Y_{BCO}) and bio-pyrolysis gas (Y_{BPG}) [42]. If BPG consists of H_2O, CO_2, CO, H_2, and CH_4, the Y_{VY} value is then similar to the summation of each volatile product component, as seen in Eq. 6. The actual yield of each component (Y_i) is the ratio between mass of each component (m_i) and mass of oil palm shell (m_{OPS}). The value is equal to the multiplication product of actual mass fraction of each component (y_i) with Y_{VY} as described in Eq. 7.

$$Y_{VY,p} = e^{f_5\left(\frac{T}{T_s}\right)}.Y_{VM,p} \tag{4}$$

$$f_5\left(\frac{T}{T_s}\right) = 6153.35\left(\frac{T}{T_s}\right)^5 - 17139.90\left(\frac{T}{T_s}\right)^4 + 18990.22\left(\frac{T}{T_s}\right)^3 - 10506.63\left(\frac{T}{T_s}\right)^2 + 2934.34\left(\frac{T}{T_s}\right) - 338.05 \tag{5}$$

$$Y_{VY} = Y_{BCO} + Y_{BPG} = Y_{BCO} + Y_{H_2O} + Y_{CO_2} + Y_{CO} + Y_{H_2} + Y_{CH_4} \tag{6}$$

$$Y_i = \frac{m_i}{m_{OPS}} \times 100\% = y_i.Y_{VY} \tag{7}$$

The model transformation from solid-state to volatile state approach is given in Table 1 where the conversion function (α) is replaced by Y_{VY}. The predicted yield ($Y_{i,p}$) and predicted mass fraction ($y_{i,p}$) of each

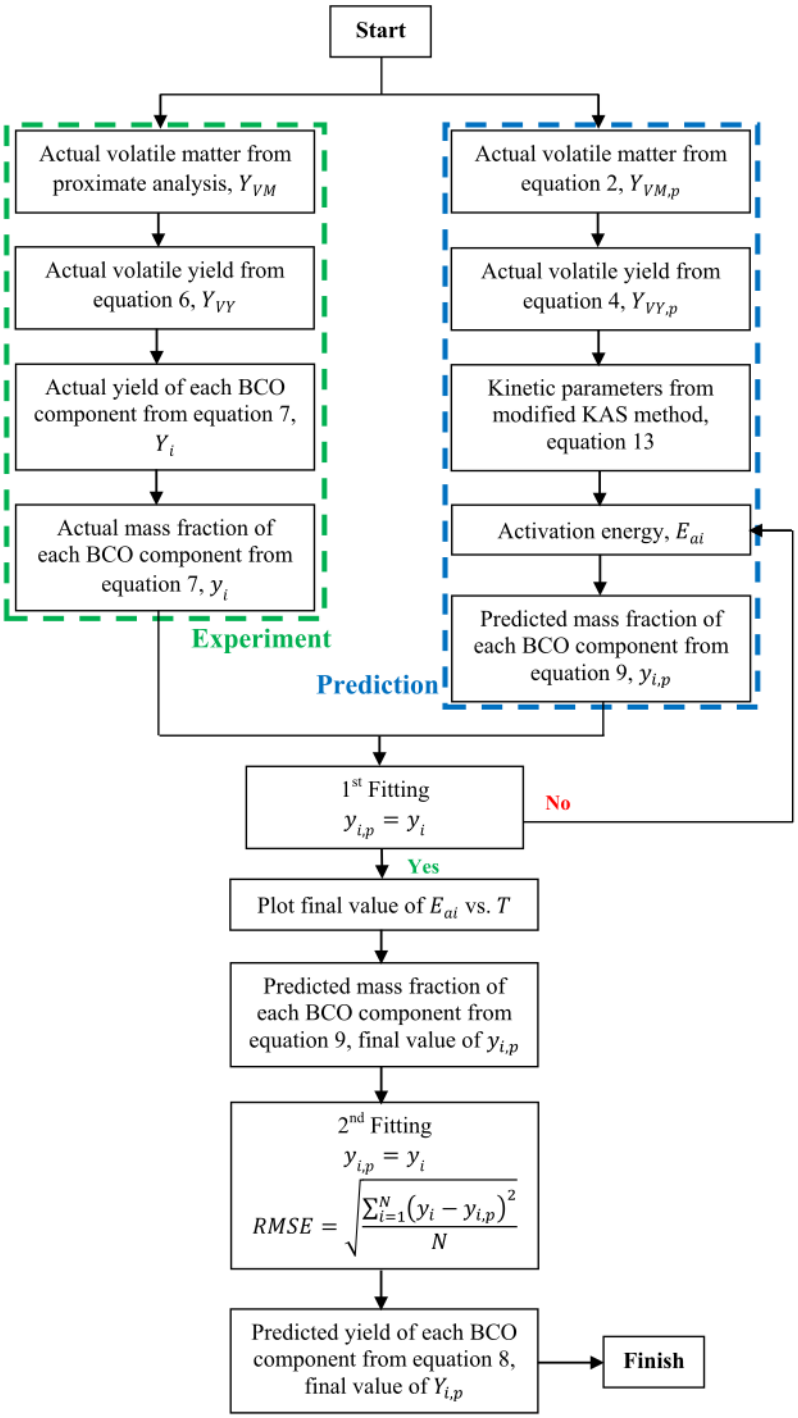

Fig. 1. The flowchart to predict mass fraction, yield, and to determine kinetic parameters of each BCO component.

Table 2
Oil palm shell physicochemical properties.

Parameter	Units	Value
Biomass Type Number (N_{CT})	–	9.57
Volatile Matter (Y_{VM})	%-wt	71.90
Fixed Carbon	%-wt	18.26
Ash Content	%-wt	2.23
Moisture Content	%-wt	7.61
C	%-wt	49.51
H	%-wt	6.18
O	%-wt	41.45
N	%-wt	2.86

component are shown in Eqs. 8 and 9. The ratio of the experimental and predicted mass fraction will then specify the activation energy of each volatile component which is expressed as temperature function.

$$Y_{i,p} = y_{i,p}.Y_{VY,p} \tag{8}$$

$$y_{i,p} = \frac{A_i}{\beta} e^{-f_5\left(\frac{T}{T_f}\right)} \int_{T_0}^{T} \left[e^{\left(\frac{-E_{ai}}{RT}\right) - f_2(N_{CT})} - e^{\left(\frac{-E_{ai}}{RT}\right) + f_5\left(\frac{T}{T_f}\right)} \right] .dT \tag{9}$$

where A_i is Arrhenius constant of each component (min^{-1}), β is heating rate, (°C/min), E_{ai} is activation energy of each component (J/mol), T_0 is initial temperature (K) where the product has not been formed, T is instantaneous pyrolysis temperature (K), and R is ideal gas constant (8.314 J/mol/K).

One of the widely-known and established kinetic models is the Kissinger-Akahira-Sunose (KAS) which is derived from the solid-state approach [13]. This model is then modified to a volatile state basis as expressed in Eq. 10. Hereafter, combining Eq. 10 and Eq. 4 generates the modified KAS method, Eq. 11. Taking integration of the two sides of Eq. 11 leads to Eq. 12. Eq. 12 should then be linearized in order to obtain the kinetic parameters. Linearization is realized by applying a natural logarithm, as seen in Eq. 13. If $\frac{2RT}{E_a} << 1$, the value could be neglected. Finally, the slope of the plot between $ln\left(\frac{\beta}{T^2}\right)$ versus $\frac{1}{T}$ will lead to activation energy determination.

$$\frac{dY_{VY,p}}{1 - Y_{VY,p}} = \frac{A}{\beta} e^{\left(\frac{-E_a}{RT}\right)} .dT \tag{10}$$

$$\int_{T_0}^{T} \frac{d\left[e^{f_5\left(\frac{T}{T_f}\right) + f_2(N_{CT})}\right]}{1 - e^{f_5\left(\frac{T}{T_f}\right) + f_2(N_{CT})}} = \int_{T_0}^{T} \frac{A}{\beta} e^{\left(\frac{-E_a}{RT}\right)} .dT \tag{11}$$

$$\frac{\beta}{T^2} = \frac{A.R.\left[1 - \frac{2RT}{E_a}\right].e^{\left(\frac{-E_a}{RT}\right)}}{-ln\left[1 - e^{f_5\left(\frac{T}{T_f}\right) + f_2(N_{CT})}\right].E_a} \tag{12}$$

$$ln\frac{\beta}{T^2} = ln\left[\frac{A.R}{-ln\left(1 - e^{f_5\left(\frac{T}{T_f}\right) + f_2(N_{CT})}\right).E_a}\right] - \frac{Ea}{\mathrm{RT}} \tag{13}$$

The procedure to predict mass fraction, yield, and to determine kinetic parameters of each BCO component, as has previously been described, following the flowchart in Fig. 1, but it is suggested to initially classify the variables for experiment and prediction. The variables for experiment are Y_{VM} from proximate analysis, Y_{VY} from Eq. 6 as well as y_i and Y_i from Eq. 7. On the other hand, the variables for prediction include $Y_{VM,p}$ from Eq. 2, $Y_{VY,p}$ from Eq. 4, E_{ai} from Eq. 13, $y_{i,p}$ from Eq. 9, and $Y_{i,p}$ from Eq. 8. All the variables that related to the experiment were calculated at first. The $Y_{VM,p}$ and $Y_{VY,p}$ were then calculated to get the first value of E_{ai} and continued to straight forward calculation for obtaining the first value of $y_{i,p}$.

The value of $y_{i,p}$ from the first trial was compared to y_i. The first fitting, by means of 100 iterative calculations, was then performed until the ratio between these two variables was 1. The final value of E_{ai} value from the first fitting was plotted versus temperature to get the second-order polynomial function. This function was substituted to Eq. 9 for

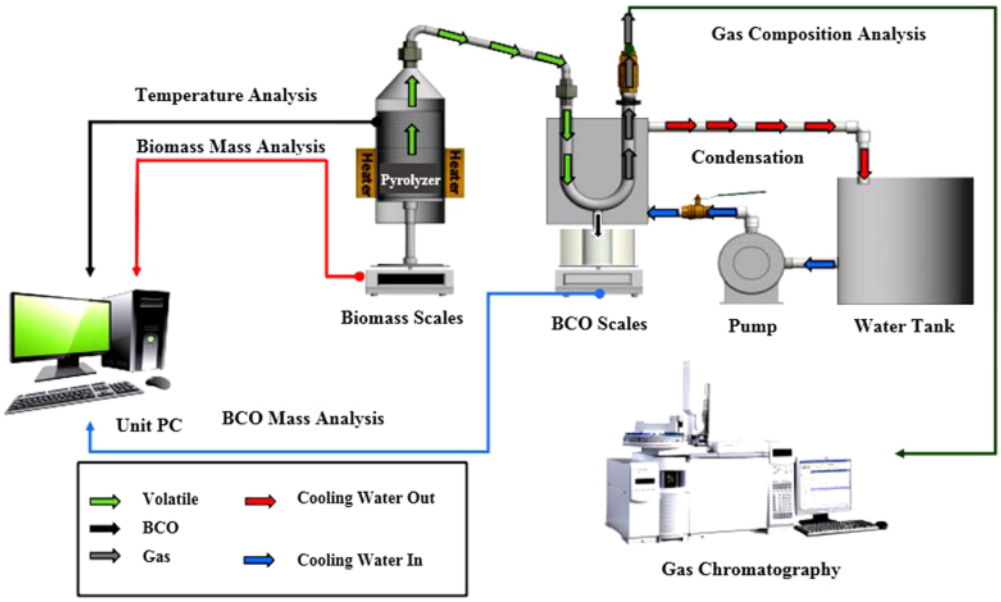

Fig. 2. Pyrolysis production analysis thermal gravimetry (PPA-TG) apparatus.

acquiring the final value of $y_{i,p}$. The discrepancy of y_i and $y_{i,p}$ must comply with the root mean square error (RMSE) of below 0.5% in order to achieve result validation [17]. The final value of $y_{i,p}$ was then used in Eq. 10 for gaining the final value of $Y_{i,p}$.

2.2. Experimental section

The oil palm shell was acquired from PT. Perkebunan Nusantara VIII Lebak, Banten with the proximate and ultimate analysis as outlined in Table 2. Pretreatment by screening from soil and rock was done using a mesh filter to separate the small size impurities. The oil palm shell was then dried for 72 h and was ground until the size reach 10 mesh. After that, 300 g of ground oil palm shell was then pyrolyzed in a semi-batch mode. This is none other than a batch mode pyrolysis with the presence of volatile products outflow.

The pyrolysis was carried out under the apparatus named pyrolysis production analysis thermal gravimetry (PPA-TG). It has a 4-inch diameter tube embedded with a temperature measuring device, as shown in Fig. 2. This apparatus was also equipped with analytical scales with a capacity of 3000 ± 0.1 g to measure the mass loss as well as the BCO formation. In order to scale up the production capacity, a larger and more precise analytical scale is recommended to be utilized.

In the PPA-TG apparatus, pyrolysis was done at 300 °C, 350 °C, 400 °C, 450 °C, and 500 °C and the heating rate was set manually at 6 °C/min. The data collection for oil palm shell mass loss as well as BCO mass formation were performed automatically using GenWeigh (Ind. A12E) software for better measurement and data processing accuracy. The principle of the mass loss in the reactor was explained using the floating dome concept by pushing the reactor upward as a result of the volatile matter production that flows into the condenser. The data collection was terminated when there were no more drops produced from the condenser pipeline.

2.3. Chemicals characterization

The biomass moisture content analysis was done in a special oven drying (followed ASTM D-2173), volatile matter measurement in a special furnace (followed ASTM D-3175), ash content determination in a muffle furnace (ASTM D-3174), and fixed carbon calculation by difference (followed ASTM D-3172). Other than that, the biomass ultimate analysis was carried out under CHN 628 determinator equipped with an infrared detector for C and H elements as well as a thermal conductivity detector for N element. The procedure followed ASTM D-5373.

The ultra-performance liquid chromatography with photodiode array detector (UPLC-PDA) analysis was purposed to measure carbohydrate compounds. The instrument employs a C18 column (inner diameter 3 mm) with 0.02 mol/L of phosphoric acid as a mobile phase, an isocratic flowrate of 0.425 mL/min, and 10% acetonitrile for needle wash. As much as 0.5 g of organic acid was used as a standard. The standard was sonicated, added with 0.02 mol/L phosphate buffer, and was filtered before entering the UPLC-PDA instrument. The sample (2 mL) was initially mixed with 5 mL of 0.02 mol/L phosphate buffer. About 10 min of sonication was then applied and further was followed by centrifugation under 4000 rpm for 10 min. After sample preparation, the column should be conditioned with 1.5 mL of methanol and was followed by bi-cleaning with 1 mL of 0.02 mol/L phosphate buffer. As much as 2.5 mL of supernatant from previous sample centrifugation then flowed to the column and the outlet was filtered. The filtered sample's supernatant was finally injected into the instrument for analysis.

The gas chromatography flame ionization detector (GC-FID) analysis was performed to determine the fatty acid compounds. The used standard was 10 mL of diluted FAME C_6-C_{24} with n-hexane. The sample should be initially well-mixed with isopropanol, 6 mL n-hexane, and 3 mL demineralized water. The substance in the top layer was collected

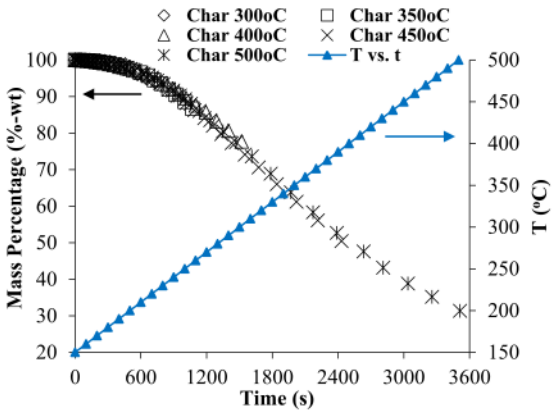

Fig. 3. Mass loss evolution of oil palm shell pyrolysis.

and the remaining solvent was evaporated. The extracted sample was then methylated with 1.5 mL of 0.5 mol/L KOH at 100 °C. Additionally, the solution was cooled, added with 20% BF_3, and heated again at 100 °C. The cooled solution was mixed with 3 mL of saturated NaCl solution and 2 mL n-hexane. Again, the substance in the top layer was separated and directly mixed with anhydrous Na_2SO_4. Subsequently, 1 μL of the methylated sample was injected into a Perkin Elmer Clarus 580 GC-FID instrument at 225 °C. Nitrogen was assisted as a carrier gas and the capillary column used was Supleco SP™ 2560. The FID detector was operated at 240 °C with H_2 flow of 45 mL/min and air flow of 450 mL/min. The recorded peak of the chromatogram belongs to the C_{24} fatty acids in the sample comparing their retention time with the retention time of the standard.

Folin-Ciocâlteu analysis was intended to identify the total phenol amount contained in the BCO. The reaction between this reagent and phenol compound will form a blue substance. The darker color indicated the higher phenol amount. The sample (50 g) was initially mixed with 2.5 mL of 95% ethanol and 1 mL of the previous solution was supplemented with 1 mL ethanol, 5 mL of demineralized water, and 0.5 mL of Folin-Ciocâlteu reagent. After 5 min, 1 mL of Na_2CO_3 was added and the solution was vortexed. The solution was held in the darkroom for 40 min and the phenol concentration measurement was aided by a spectrophotometer under a wavelength of 725 nm.

An Agilent GC7890A-MS5975C of gas chromatography-mass spectrometer (GC-MS) instrument equipped with an electron ionization detector was applied for aromatic compound analysis. The oven temperature was programmed at 40 °C for 2 min, then increased by 5 °C/min to 70 °C, then escalated by 20 °C/min to 280 °C, and raised again by 30 °C/ min to 299 °C and held for 3 min. Inlet condition was set at 250 °C, split mode ratio 5:1, volume 1 L, flowrate 4.5 mL/min, and pressure 5.9529 psi. The MS detector was set with solvent delay 2.60 min, mass scan mode 40–550, ion source 230 °C, quadrupole 150 °C. The column 5%-phenyl-methylpolysiloxane with an inner diameter of 0.25 mm and length 30 m was used as a stationary phase, while helium with 99.999% purity was used as a mobile phase. An analytical grade of 2 g/L BTEX (benzene, toluene, ethylbenzene, xylene) was diluted in a volumetric flask using n-hexane until reaching 0.4–8.0 mg/L. This solution was injected and analyzed as a standard. The sample was mixed with n-hexane and was then sonicated for 5 mins at room temperature. After sonication, the mixture was filtered using a PTFE syringe filter with a pore size of 0.22 m. The sample solution was then injected and analyzed. Data interpretation refers to the Willey 09 and NIST 08 Library/Database.

The amount of water content in BCO was recorded by moisture meter Karl-Fischer 31 instrument which applied volumetric titration. The

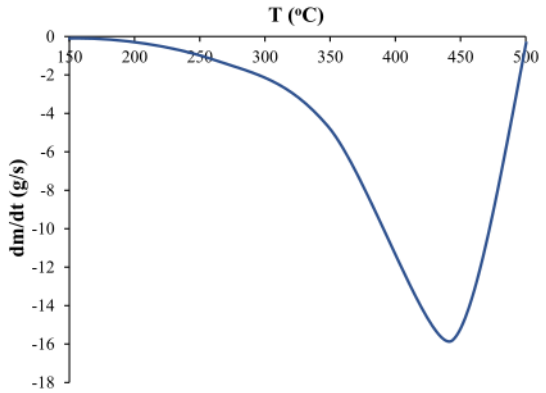

Fig. 4. Derivative mass loss of oil palm shell pyrolysis.

other materials involved were GEX/OL II/KTX as a solvent, 3 g/L of water as a titrant, and demineralized pure water as a standard. The electrode should be cleaned with ethanol and the drying tube must be filled with an active silica gel. The titration flask was initially filled with solvent and followed by solvent dehydration. Demineralized pure water was then injected into the titration flask for standard. Afterward, the sample with a certain amount was filled into the titration flask to be analyzed. The water content measurement was automatically calculated in the instrument.

3. Results and discussion

3.1. Oil palm shell pyrolysis performance in PPA-TG

Fig. 3 serves the mass loss evolution of oil palm shell pyrolysis for 1 h under a constant heating rate of 6 °C/min. Following this figure, the biomass devolatilization process under each pyrolysis temperature shows a similar mass loss pattern which means the apparatus has very good performance. It is also seen that oil palm shell initial mass loss under five pyrolysis temperatures starts at 160 °C. The mass loss is greater along with increasing pyrolysis temperature and reaches the final mass value at 63.42%-wt, 57.00%-wt, 49.00%-wt, 22.29%-wt, 13.29%-wt, and 6.10%-wt under pyrolysis temperatures of 300, 350, 400, 450, and 500 °C, in sequence.

For each variation, the temperature was held for 10 mins only to ensure the pyrolysis process has completely done. From the results, it turned out that holding treatment does not give a meaningful effect which is exhibited by the nearly same mass loss percentage for all pyrolysis temperatures. The recorded mass loss after 10 min of holding time under pyrolysis temperatures of 300, 350, 400, 450, and 500 °C are 0.52%-wt, 1.07%-wt, 0.99%-wt, 1.00%-wt, and 0.61%-wt, in successive terms. Likewise, the BCO compounds begin to form at 450 and 500 °C due to their significant mass losses. This is reinforced by the appearance of data points that are getting farther away from each other which implies the optimal temperature for BCO formation.

Apart from that, the derivative mass loss of oil palm shell pyrolysis in Fig. 4 obviously reveals the presence of one peak which reflects that only the primary reaction occurs. Furthermore, this study employs the small size of biomass particles (10 mesh) as well as utilizing the volatile fast-condensation making volatile residence time in the PPA-TG apparatus becomes low [43]. The aforementioned facts clearly reinforce that further BCO cracking, as a secondary reaction, can be completely ignored [31]. Moreover, the secondary reaction in the oil palm shell and wood slow pyrolysis was observed at 600 °C [44,45] whereas this study only up to 500 °C.

3.2. Qualitative analysis of BCO components

In pursuance of the GC-MS result (Fig. 5), the pyrolysis at 500 °C successfully produced BCO which contains 72.79%-wt water and 27.21%-wt organic compounds. The BCO consists of 95 compounds as

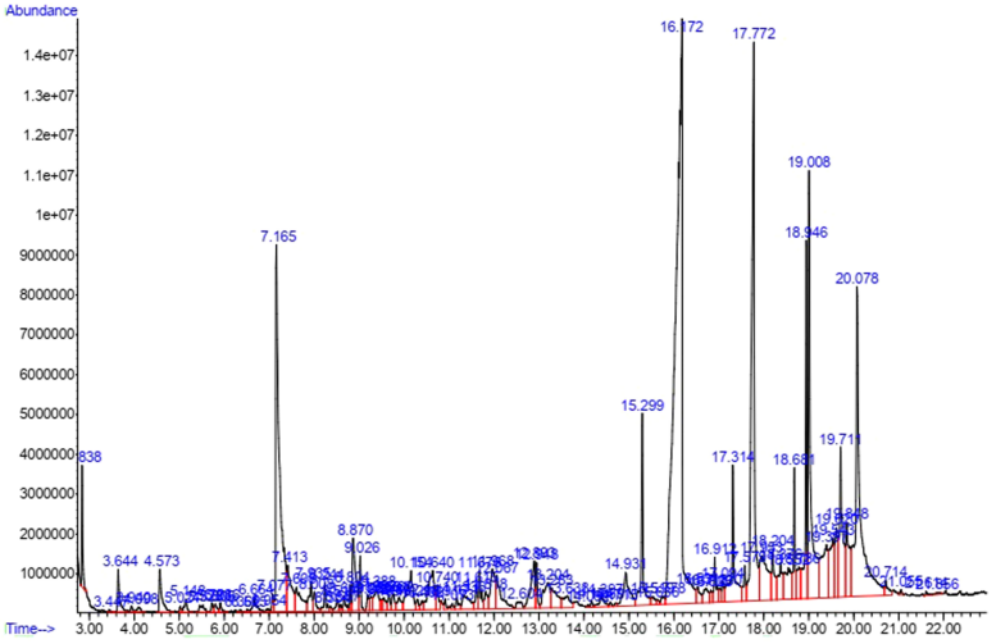

Fig. 5. Chromatogram profile for BCO product.

Table 3
BCO composition under pyrolysis at 500 °C.

No.	Components	Area (%)	Retention Time (min)
1.	2-Methyltetrahydrofuran	0.02	3.45
2.	Toluene	0.49	3.64
3.	1-Methyl-1-Ethylcyclopropan	0.06	3.94
4.	(3e,5e)-Hepta-3,5-Dien-2-One	0.09	4.10
5.	Furfural	0.66	4.57
6.	Ethylbenzene	0.05	5.02
7.	Xylene	0.20	5.15
8.	P-Xylene	0.20	5.53
9.	2-Methyl-2-Cyclopentenone	0.10	5.73
10.	2-Isopropylfuran	0.13	5.81
11.	Anisole	0.12	5.92
12.	2,3-Dimethyl-2,4-Hexadiene	0.04	6.36
13.	N-Propylbenzene	0.03	6.52
14.	5-Methyl Furfural	0.29	6.66
15.	M-Ethylmethylbenzene	0.05	6.95
16.	N-1-Decene	0.16	7.08
17.	Monophenol	7.53	7.17
18.	Phenol	1.16	7.41
19.	Formic Acid Phenyl Ester	0.86	7.61
20.	2,3-Dimethyl-2-Cyclopenten-1-One	0.48	7.94
21.	4-Hydroxybenzaldehyde	0.30	8.01
22.	Hydroxybenzene	0.32	8.24
23.	Benzene	0.06	8.36
24.	Bicyclo[1,3]Heptan-2-One	0.16	8.51
25.	3-Methylpyridazine	0.07	8.59
26.	1-Undecene	0.20	8.67
27.	Methyl Ester Benzoic Acid	0.22	8.80
28.	Guaiacol	1.40	8.87
29.	2-Methyl Benzofuran	0.45	9.03
30.	O-Cresol	0.19	9.20
31.	2-Methyl Fenol	0.18	9.27
32.	P-Cresol	0.59	9.39
33.	O-Hydroxy Toluene	0.13	9.49
34.	M-Cresol	0.23	9.55
35.	3-Methyl-1 h-Indene	0.19	9.66
36.	4-Methyl Fenol	0.27	9.76
37.	4-Cresol	0.31	9.89
38.	Caprylic Acid	1.18	10.15
39.	3-Methyl Fenol	0.15	10.30
40.	3-Hydroxy Benzene Ethanol	0.12	10.40
41.	2-Methoxy-4-Methyl Phenol	1.38	10.64
42.	2-Methoxy-P-Cresol	0.32	10.74
43.	3,4-Dimethoxytoluene	0.11	10.92
44.	1,7,7-Trimethyl-2-Methylenebicyclo	0.07	11.07
45.	P-Tert-Butyl Phenol	0.17	11.17
46.	2,6-Dimethyl Phenol	0.60	11.34
47.	2,3-Dihydro-1 h-Inden-1-One	0.27	11.62
48.	2-Undecanone	0.46	11.68
49.	1-Methyl-Naphthalene	0.33	11.82
50.	4-Ethyl-2-Methoxy Phenol	1.02	11.97
51.	4-Ethylguaiacol	0.96	12.07
52.	2-Methoxy-4-Vinylphenol	0.21	12.60
53.	Capric Acid	1.09	12.89
54.	4-Methoxy-Benzoic Acid Methyl Ester	0.42	12.95
55.	Eugenol	0.91	13.20
56.	2,6-Dimethoxy Phenol	0.74	13.28
57.	2-Methoxy-4-Propyl Phenol	0.50	13.63
58.	3-Hexadecyne	0.03	14.09
59.	Indole-7-Carboxaldehyde	0.06	14.17
60.	Trans-M-Propenyl Guaiacol	0.31	14.40
61.	4,4a,5,6,7a,8-Hexahydro-7 h-Indeno[5,6-B]Furan-7-One	0.05	14.59
62.	2,3,4-Trimethyl-5-(1-Methylallyl) Cyclopentadiene	0.05	14.72
63.	Cis-Isoeugenol	1.14	14.93
64.	Methyl Laurate	2.03	15.30
65.	1,2,4-Trimethoxybenzene	0.18	15.52
66.	2-Hydroxy-5-Methyl-1,3-Benzenedimethanol	0.07	15.64
67.	5-Hydroxy-2-Methoxy-Benzoic Acid Methyl Ester	0.16	15.78
68.	Lauric Acid	22.81	16.17
69.	2-Allyl-1-Methylnaphthalene	0.34	16.53

Table 3 (*continued*)

No.	Components	Area (%)	Retention Time (min)
70.	1-Phenyl-1-Penten-5-Ol	0.42	16.72
71.	4-Hydroxyphthalic Acid	0.17	16.83
72.	8-Heptadecene	0.54	16.91
73.	9-Octadecenoic Acid	0.19	17.03
74.	14-Methyldotriacontane	0.22	17.09
75.	Methyl Tetradecanoate	2.13	17.31
76.	4-Methoxy-6-(2-Oxopropyl)- 2 h-Pyran-2-One	0.43	17.58
77.	Myristic Acid	8.84	17.77
78.	Tetradecanoic Acid	2.06	17.95
79.	1-Acetoxy-3-Phenyl-3-Phenoxyaceton	0.80	18.20
80.	Oleic Acid	0.86	18.38
81.	9-Octadecenoic Acid	1.15	18.55
82.	Methyl Ester Hexadecanoic Acid	1.02	18.68
83.	Palmitic Acid	0.67	18.79
84.	3,6-Dipropyl-1,2-Dihydro-1,2,4,5-Tetrazine	2.76	18.95
85.	Palmitic Acid	5.69	19.01
86.	Oleic Acid	2.10	19.40
87.	Cis-13-Octadecenoic Acid	1.50	19.54
88.	Cis-Vaccenic Acid	1.05	19.62
89.	Methyl Ester Oleic Acid	2.73	19.71
90.	Trans-13-Octadecenoic Acid	1.55	19.85
91.	Oleic Acid	8.08	20.08
92.	9-Octadecenoic Acid	0.27	20.71
93.	6-Octadecenoic Acid	0.05	21.06
94.	2-Methyl-Z,Z-3,13-Octadecadienol	0.04	21.62
95.	2-Octyl-Cyclopropaneoctanal	0.06	21.86

tabulated in Table 3. Di Blasi et al. [20] stated that maximum yield of BCO is formed along with the higher temperature as long as pyrolysis temperature is still below 427 °C. This occurs because the reaction is controlled by the slow pyrolysis phenomena, whereas at high temperatures is dominated by heat transfer [20].

As a comparison, Huang et al. [46] obtained 30 components in BCO from oil palm kernel shell pyrolysis [46] whereas Kim et al. [47] analyzed the BCO components from oil palm shell fast pyrolysis at a temperature of 450 °C and has succeeded to identify 23 compounds [47]. Khor et al. [48] displayed the composition of BCO from the empty palm fruit bunch pyrolysis consisting of 19 compounds which occupied as many as 89.42%-wt and the remaining 10.58%-wt have not been identified yet [48]. Other researchers have also found and identified 40 organic compounds in BCO from beech wood pyrolysis [40], 17 compounds in BCO from hazelnut shell pyrolysis [49], 37 organic compounds in BCO from beech, spruce, olive husk, and hazelnut shell pyrolysis [50], 38 components in BCO from pinewood pyrolysis [51], 39 major compounds in BCO from raspberry seed flash pyrolysis [52], and even up to 100 components of the BCO constituent derived from paulownia wood pyrolysis [53].

From those 95 compounds in the BCO, 15 of them have been successfully quantified due to their significant amount, 97%-wt. The others are considered as a minor constituent that has a less meaningful impact because only 3%-wt occupies the rest 80 compounds. The BCO components are then categorized into several groups, i.e. carbohydrate, fatty acid, phenol, and aromatic [20,40]. Meanwhile, the water produced from the pyrolysis process is set apart and not included in any group. The carbohydrates group are represented by acetic acid, fatty acid groups are reflected by C_8-C_{22} compounds, phenol groups are denoted by phenol compounds, and aromatic groups are indicated by benzene, toluene, xylene, and ethylbenzene. The aromatic compound was also identified by Huang et al. (2019) in their BCO from oil palm shell pyrolysis [46] as well as by Khor et al. [48], Khor and Lim [54], and Ruengvilairat et al. [55] from empty oil palm fruit bunch pyrolysis.

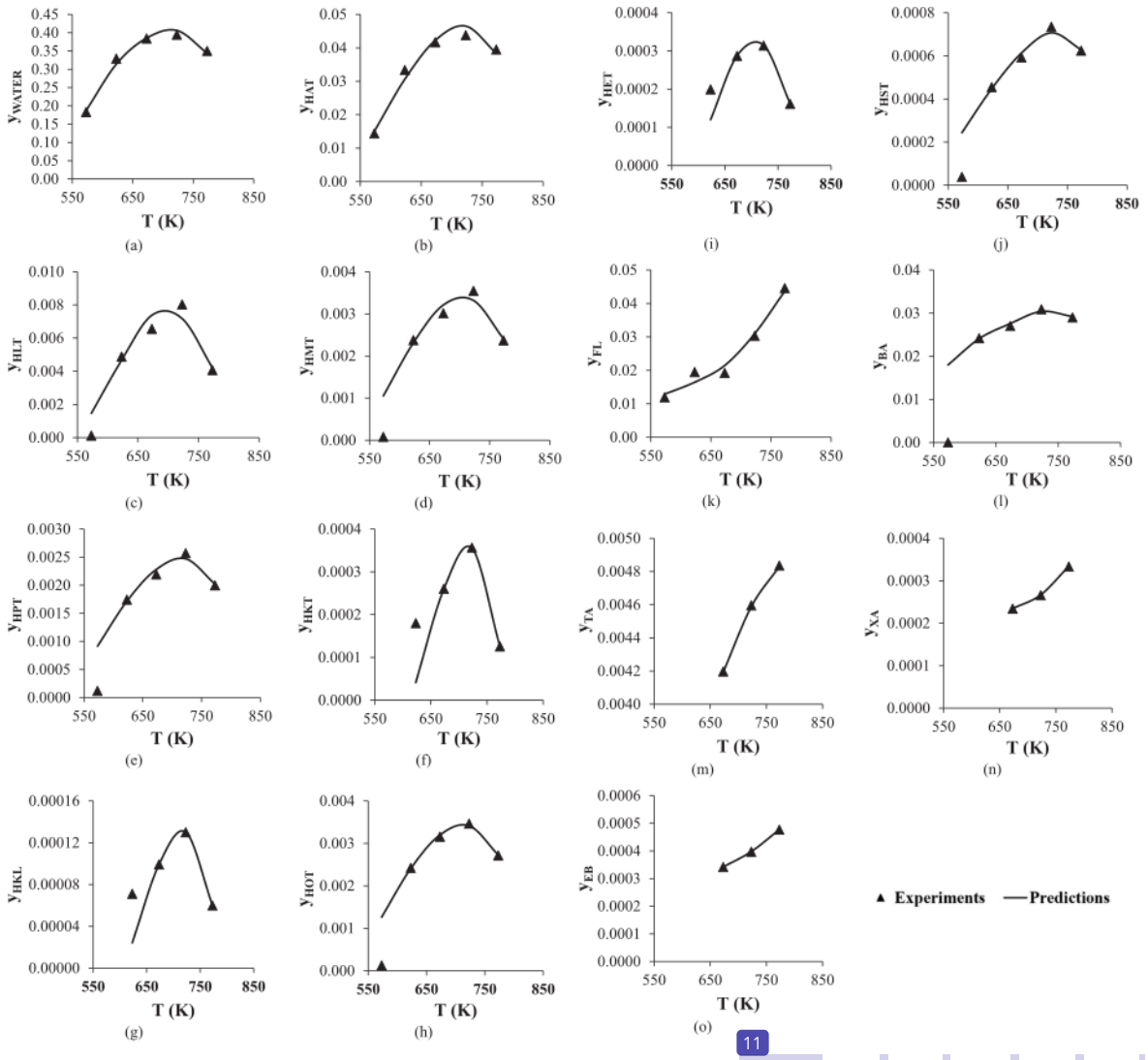

Fig. 6. Comparison between mass fraction (y_i) of BCO components from prediction vs. experimental data for water (a), HAT (b), HLT (c), HMT (d), HPT (e), HKT (f), HKL (g), HOT (h), HET (i), HST (j), FL (k), BA (l), TA (m), XA (n), and EB (o).

3.3. Mass fraction and yield prediction performance

The predicted mass fraction of each BCO component is depicted in Fig. 6. Under all pyrolysis temperatures, it has close results to the experiment. Fatty acid compounds such as capric acid, caprylic acid, and erucic acid are produced significantly at 400 °C. Benzene in BCO also dominates as an aromatic compound group at a temperature of 350 °C whereas other aromatic groups like toluene, xylene, and ethylbenzene are less produced. Also, water, stearic acid, and fatty acid compound groups have already reached their peak conditions. In contrast, a different pattern is exhibited for phenolic and aromatic groups which are still allowed to increase along with enhancing temperature.

A similar result to Branca et al. [56] is found where the phenol formation tends to enhance at 327–627 °C with the absence of decreasing yield [56]. However, there is a difference between predicted and experiment mass fraction under pyrolysis at 300 °C for five fatty acid compounds such as lauric acid, myristic acid, palmitic acid, oleic acid, and stearic acid. At this temperature, the values are extremely low or can be neglected. The same phenomenon was found in the study from Aziz et al. [57] which denoted the product from the empty palm fruit bunches, oil palm shell, and oil palm husk torrefaction at a reaction temperature of 200–300 °C was dominated by light gas (CO, H_2, CH_4, CO_2) while fatty acids as a liquid product were obtained lesser [57]. Even so, the volatile state approach is still able to predict the mass fraction of each BCO component with a good similarity to the experimental data at a temperature of more than 300 °C.

Besides, Fig. 7 describes the predicted yield for each BCO component under all temperatures which are in good agreement with the experiment. In accordance with Eq. 8, the predicted yield of each BCO component is calculated from the multiplication of the predicted mass fraction of each BCO component and the predicted volatile yield. Multiplication operation augments the values of predicted yield and as a result, the values are slightly closer to the experimental data rather than the predicted mass fraction.

Every drop of BCO that flows out from the bottom of the condenser has a black color which is then collected in a beaker glass attached to the

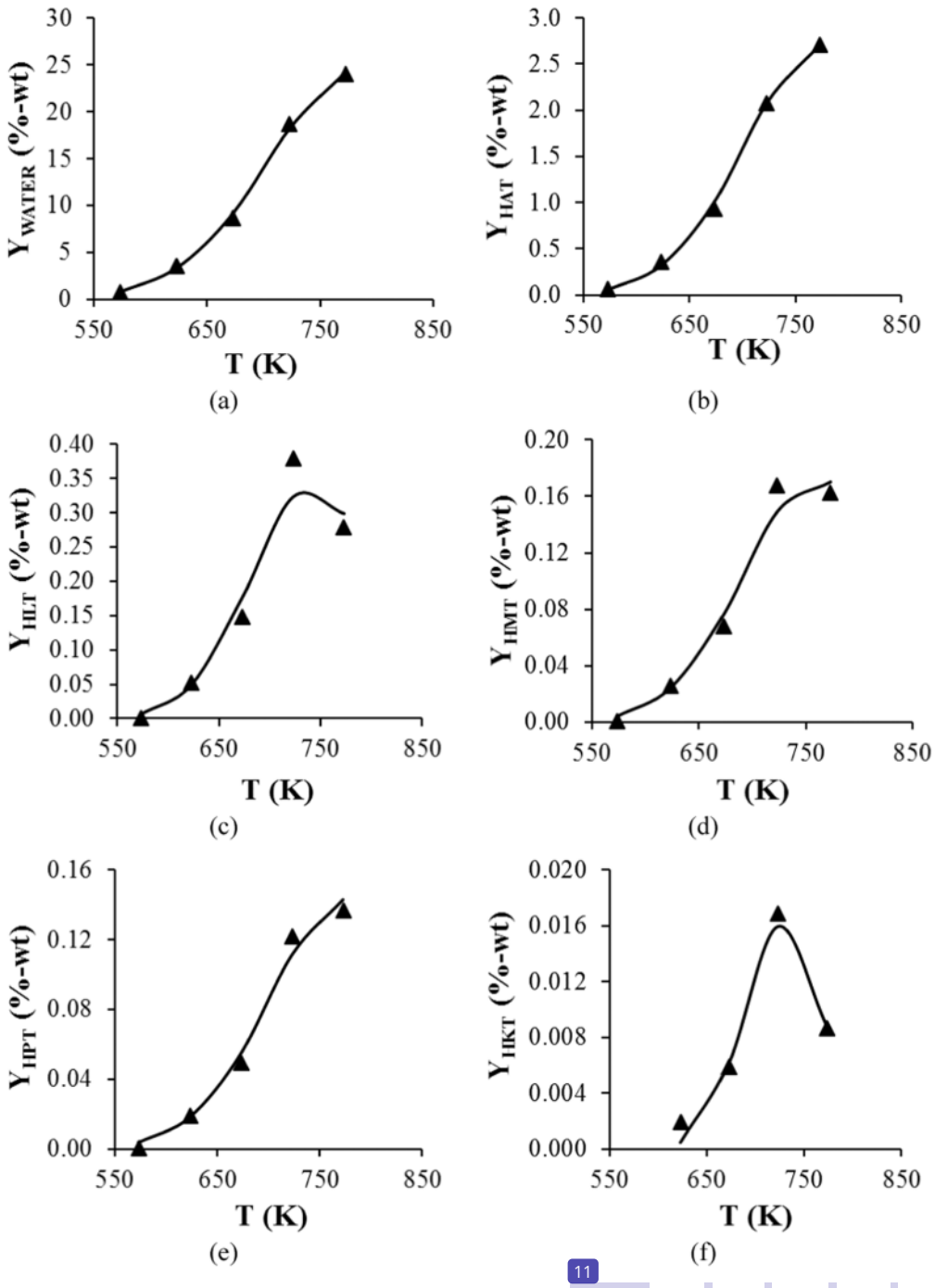

Fig. 7. Comparison between yield (Y_i) of BCO components from prediction vs. experimental data for water (a), HAT (b), HLT (c), HMT (d), HPT (e), HKT (f), HKL (g), HOT (h), HET (i), HST (j), FL (k), BA (l), TA (m), XA (n), and EB (o).

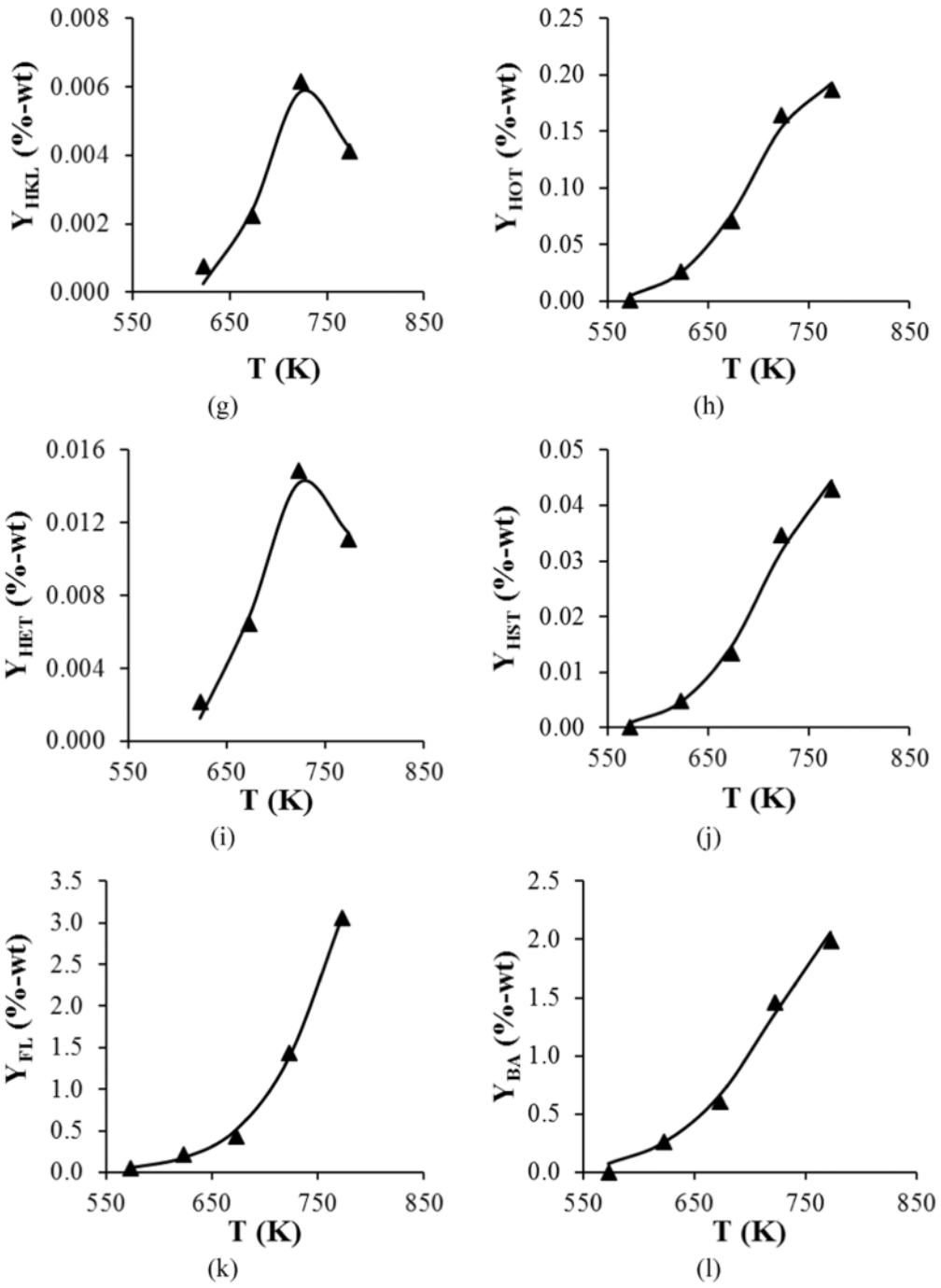

Fig. 7. (*continued*).

PPA-TG apparatus. The water (aquatic phase) naturally separates from the organic phase. The aquatic phase is thinner, clearer, and floats to the top surface, while the organic phase appears thick dark black and sediments to the bottom surface. The dominating upper layer implies that water occupies the largest compound in the BCO from oil palm shell pyrolysis. This qualitative evidence is strengthened by the results that water occupies 72.79%-wt. The major products are then followed by phenol, acetic acid, and benzene. Table 4 shows the yield of 15 BCO components from pyrolysis at 500 °C. All of the predicted yield values are quite similar, even having RMSE below 0.5%, to the experimental yield. This indicates that volatile state approach has an excellent prediction accuracy.

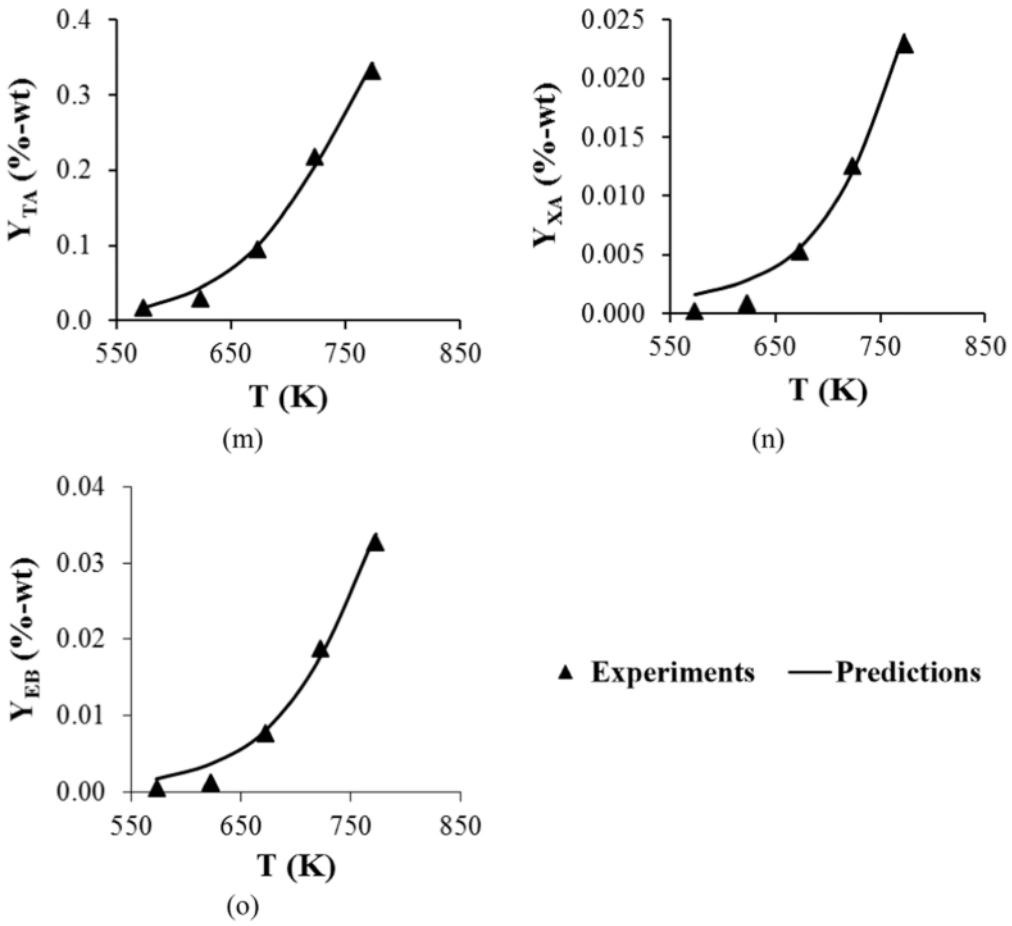

Fig. 7. (*continued*).

Table 4
The yield (Y_i) of 15 BCO components under pyrolysis at 500 °C.

No.	BCO components	Predicted yield (%-wt)	Experimental yield (%-wt)	RMSE (%)
1.	Water	24.35	24.04	0.22
2.	Phenol (FL)	3.09	3.06	0.02
3.	Acetic Acid	2.72	2.71	0.01
4.	Benzene (BA)	2.07	1.99	0.06
5.	Toluene (TA)	0.34	0.33	0.01
6.	Lauric Acid (HLT)	0.30	0.28	0.01
7.	Oleic Acid (HOT)	0.19	0.19	0.00
8.	Miristic Acid (HMT)	0.17	0.16	0.01
9.	Palmitic Acid (HPT)	0.14	0.14	0.00
10.	Stearic Acid (HST)	0.04	0.04	0.00
11.	Ethylbenzene (EB)	0.03	0.03	0.00
12.	Xylene (XA)	0.02	0.02	0.00
13.	Erucic Acid (HET)	0.011	0.023	0.01
14.	Capric Acid (HKT)	0.009	0.011	0.00
15.	Caprylic Acid (HKL)	0.004	0.004	0.00

3.4. Pyrolysis kinetic parameters

The oil palm shell mass loss data is used for determining the kinetic parameters (Arrhenius constant and activation energy) which employ the modified KAS method. The determination is done through fitting as were also carried out by other researchers [13,58]. Under conventional fitting procedure, which is widely carried out by straight-line extrapolation of experimental data, the obtained activation energy is always constant which has generally been known [59]. Contrary to the two-step-fitting procedure, as applied in this study, the non-linear line is plotted as close as possible to the experimental data points. As a consequence, the activation energy is not constant and extremely sensitive to temperature change [58]. After two-step-fitting, the results for kinetic parameters of 15 BCO components are served in Table 5.

The activation energy of each product formation is temperature dependence as a second-order polynomial function in the mathematical form of $\phi.T^2+\chi.T+\delta$ as plotted in Fig. 8. For comparison, Font et al. (1990) succeeded to analyze the temperature dependence of activation energy for liquid and gas products (H_2, CO, CO_2, and CH_4) from almond shell pyrolysis at 400–460 °C. The activation energy of each component was fitted where the value enlarges at 400–440 °C and then followed by decreasing value until 460 °C. This pattern is compatible with the second-order function and also follows the first-order pseudo-kinetic [36]. Yet, there are several complex reactions regarding activation energy as a polynomial function that has maximum and minimum values,

Table 5
Kinetic parameters for 15 BCO components.

No.	BCO Components	A (min^{-1})	$E_a = \phi.T^2 + \chi.T + \delta$ ($J.mol^{-1}$) T in K
1.	Water	8.38×10^{11}	$\phi = 0.061$ $\chi = 69.038$ $\delta = 96{,}147.797$
2.	Acetic Acid (HAT)	8.38×10^{11}	$\phi = 0.128$ $\chi = -13.003$ $\delta = 132{,}712.029$
3.	Lauric Acid (HLT)	8.38×10^{11}	$\phi = 0.410$ $\chi = -377.543$ $\delta = 260{,}051.691$
4.	Miristic Acid (HMT)	8.38×10^{11}	$\phi = 0.209$ $\chi = -97.051$ $\delta = 166{,}945.816$
5.	Palmitic Acid (HPT)	8.38×10^{11}	$\phi = 0.110$ $\chi = 38.291$ $\delta = 122{,}522.080$
6.	Capric Acid (HKT)	8.38×10^{11}	$\phi = 1.413$ $\chi = -1791.289$ $\delta = 775{,}309.293$
7.	Caprylic Acid (HKL)	8.38×10^{11}	$\phi = 1.024$ $\chi = -1235.540$ $\delta = 582\,645.948$
8.	Oleic Acid (HOT)	8.38×10^{11}	$\phi = 0.125$ $\chi = 16.378$ $\delta = 128{,}677.222$
9.	Erucic Acid (HET)	8.38×10^{11}	$\phi = 0.695$ $\chi = -762.720$ $\delta = 407{,}993.865$
10.	Stearic Acid (HST)	8.38×10^{11}	$\phi = 0.067$ $\chi = 101.722$ $\delta = 106{,}507.865$
11.	Phenol (FL)	8.38×10^{11}	$\phi = -0.246$ $\chi = 482.367$ $\delta = -27{,}722.715$
12.	Benzene (BA)	8.38×10^{11}	$\phi = 0.008$ $\chi = 154.404$ $\delta = 77{,}069.840$
13.	Toluene (TA)	8.38×10^{11}	$\phi = -0.192$ $\chi = 453.568$ $\delta = -23{,}538.383$
14.	Xylene (XA)	8.38×10^{11}	$\phi = -0.384$ $\chi = 739.618$ $\delta = -113{,}664.636$
15.	Ethylbenzene (EB)	8.38×10^{11}	$\phi = -0.304$ $\chi = 623.385$ $\delta = -73{,}370.929$

such as in epoxy-amine cure kinetic [60,61], fatty acid polymerization kinetic with maleic anhydride as acidic initiator [62], humins cross-linking reactions kinetic [63], and relaxation and glass transition kinetic for semi-crystalline poly(ethylene 2,5-furan-dicarboxylate) [64].

Indeed, the results will unsettle some kineticists. Nevertheless, it should be noted the established solid-state approach which was developed from homogeneous gas-phase reaction has a constant value of kinetic parameters and inconsistent kinetic law due to changing temperature and coordinates of reaction [65–67]. The iso-conversional kinetic concept also reveals that solid-state approach is more complex due to multi-step reactions [58,65]. Moreover, the strong dependence of activation energy with temperature and coordinates of reaction for biomass pyrolysis is due to the altering biomass physicochemical properties under high temperature, product formation phenomena, biomass crystalline structure defects, as well as intra-crystalline strain in the cellulose components [68].

In order to reconvince the calculated activation energy values, several results and discussions that deal with it are disclosed. The kinetic research with a constant value of activation energy is only appropriate

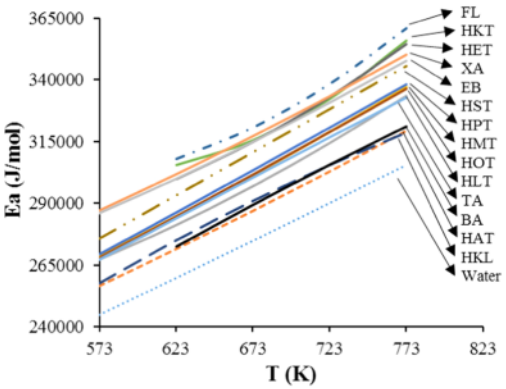

Fig. 8. The activation energy of 15 BCO components as a second-order temperature function.

for gas-phase reactions while liquid and solid reactions should engage a more complex kinetic parameter [69]. When the plot of the logarithmic value of kinetic constant vs. $\frac{1}{T}$ does not result in straight lines, it can be ascertained that multiple reactions occur by competition mechanisms and moreover, the activation energy also strongly depends on temperature change [70]. Subsequently, Moelwyn and Hughes [71] also succeeded to prove the activation energy for sucrose hydrolysis as a temperature quadratic function in the form of $\phi.T^2 + \chi.T + \delta$ with $\phi = 1.52171$, $\chi = -1019.53$, and $\delta = 193789$ [71]. The decreasing activation energy at higher temperature is due mainly to the more significant molecular mobility but it is only for non-solid complex reactions [60,61,63].

The pattern becomes contradictive when discussing the biomass pyrolysis phenomena. The moisture and volatile leaving from the biomass matrix, as a result of high-temperature exposure [5,6], yields in a more rigid biomass structure and restricts the molecular mobility which consequently intensifies activation energy value [62], as experienced in this study. Although kinetic parameters depend on temperature, the discussion has widely focused on the activation energy only. This might be due to the temperature sensitivity of the reaction rate mainly determined by the activation energy, whereas the Arrhenius factor highly relies on the activation energy which makes the effect is far more inferior [72]. In spite of that, the Arrhenius constant for oil palm shell pyrolysis from this study is still in the range with the value from wood pellet pyrolysis conducted by de Jong et al. (2003), 10^{11}–10^{16} min^{-1} [73].

4. Conclusions and prospect

The application of volatile state approach in oil palm shell pyrolysis, as well as its validation under semi-batch pyrolysis experiment, have been carried out. The pyrolysis success to produce bio-crude oil (BCO) which consists of carbohydrates, fatty acids, phenol, aromatics, and water. The carbohydrates groups are represented by acetic acid, fatty acid groups are reflected by C_8-C_{22} compounds, phenol groups are denoted by phenol compounds, and aromatic groups are indicated by benzene, toluene, xylene, and ethylbenzene. In BCO, water occupied the largest product (72.79%-wt) and was then followed by phenol and stearic acid. Besides, this study also succeeded in predicting each BCO component mass fraction and yield with reasonable and logical results compared to the experiment. The second-order polynomial equation for the temperature dependence of pyrolysis activation energy is also revealed. Finally, the robust and attractive volatile state approach is prospected to be applied to all types of biomass in order to predict their volatile mass fraction and yield.

CRediT authorship contribution statement

Pandit Hernowo: Original draft preparation; Writing – original draft; Methodology; Data curation; Visualization, **Soen Steven**: Writing – reviewing, and editing; Formal analysis; Visualization, **Elvi Restiawaty**: Supervision; Formal analysis, **Anton Irawan**: Supervision; Formal analysis; Methodology, **Carolus Borromeus Rasrendra**: Supervision; Formal analysis; Methodology, **Septhian Marno**: Validation; Resources, **Yana Meilana**: Validation; Resources, **Yazid Bindar**: Conceptualization; Supervision; Project administration.

Declaration of Competing Interest

The authors declare that they have no known competing financial interests or personal relationships that could have appeared to influence the work reported in this paper.

Acknowledgments

The study was financially supported by BPDPKS Ministry of Finance of the Republic of Indonesia and Research Trade Center PT. Pertamina. Not to forget, the authors' sincere and deep gratitude goes to Mr. Harben and Mr. Zamzami for their efforts in constructing and maintaining the PPA-TG apparatus.

References

[1] Y.W. Budhi, M. Effendy, Y. Bindar, S. Subagjo, Dynamic behavior of reverse flow reactor for lean methane combustion, J. Eng. Technol. Sci. 46 (2014) 299–317.
[2] S. Steven, E. Restiawaty, P. Pasymi, Y. Bindar, Influences of pretreatment, extraction variables, and post-treatment on bench-scale rice husk black ash (RHBA) processing to bio-silica, Asia-Pac. J. Chem. Eng. 16 (2021), e2694, https://doi.org/10.1002/apj.2694.
[3] S. Steven, Y. Ramli, D. Pratama, E. Restiawaty, Y. Bindar, Life cycle analysis (LCA) for silica production from three different routes: Conventional, fume, and green routes, In: Proceedings of the International Seminar on Chemical Engineering Soehadi Reksowardojo in conjunction with Symposium on Photocatalyst and Photocatalysis, 2020: p. 111.
[4] S. Steven, Y. Ramli, D. Pratama, E. Restiawaty, Y. Bindar, Acid wash influences on the physicochemical characteristics of bamboo leaves ash, In: Proceedings of the International Bioprocessing Association Subject Conference on Sustainable Technologies for Bioresource Utilization. Bio-Based Prod. Bioenergy, Environ. Prot., 2021: p. 124.
[5] S. Steven, E. Restiawaty, Y. Bindar, Routes for energy and bio-silica production from rice husk: A comprehensive review and emerging prospect, Renew. Sustain. Energy Rev. 149 (2021), 111329, https://doi.org/10.1016/j.rser.2021.111329.
[6] S. Steven, E. Restiawaty, Y. Bindar, Simple mass transfer simulation using a single-particle heterogeneous reaction approach in rice husk combustion and rice husk ash extraction, In: Proceedings of the International Bioprocessing Association Subject Conference on Sustainable Technologies for Bioresource Utilization. Bio-Based Prod. Bioenergy, Environ. Prot., 2021: p. 128.
[7] D.E. Rahayu, D. Nasarani, W. Hadi, B. Wrjodirjo, Potential of biomass residues from oil palm agroindustry in Indonesia, MATEC Web Conf. 197 (2018) 13008, https://doi.org/10.1051/matecconf/201819713008.
[8] T. Minowa, T. Kondo, S.T. Sudirjo, Thermochemical liquefaction of Indonesian biomass residues, Biomass Bioenergy 14 (1998) 517–524, https://doi.org/10.1016/S0961-9534(98)00006-3.
[9] X. Zhao, J. Zhang, Z. Song, H. Liu, L. Li, C. Ma, Microwave pyrolysis of straw bale and energy balance analysis, J. Anal. Appl. Pyrolysis. 92 (2011) 43–49, https://doi.org/10.1016/j.jaap.2011.04.004.
[10] M.I. Jahirul, M.G. Rasul, A.A. Chowdhury, N. Ashwath, Biofuels production through biomass pyrolysis: a technological review, Energies 5 (2012) 4952–5001, https://doi.org/10.3390/en5124952.
[11] H.B. Goyal, D. Seal, R.C. Saxena, Bio-fuels from thermochemical conversion of renewable resources, Renew. Sustain. Energy Rev. 12 (2008) 504–517.
[12] M.C.B. Lopez, C.G. Blanco, A. Martınez-Alonso, J.M.D. Tascon, Composition of gases released during olive stones pyrolysis, J. Anal. Appl. Pyrolysis. 65 (2002) 313–322, https://doi.org/10.1016/S0165-2370(02)00008-6.
[13] N. Koga, A review of the mutual dependence of Arrhenius parameters evaluated by the thermoanalytical study of solid-state reactions: The kinetic compensation effect, Thermochim. Acta. 244 (1994) 1–20, https://doi.org/10.1016/0040-6031(94)80202-5.
[14] A. Khawam, D.R. Flanagan, Solid-state kinetic models: Basics and mathematical fundamentals, J. Phys. Chem. 110 (2006) 17315–17328.
[15] M.E. Brown, A.K. Galwey, Arrhenius parameters for solid-state reactions from isothermal rate-time curves, Anal. Chem. 61 (1989) 1136–1139, https://doi.org/10.1021/AC00185A017.
[16] C.Di Blasi, Modeling and simulation of combustion processes of charring and non-charring solid fuels, Prog. Energy Combust. Sci. 19 (1993) 71–104, https://doi.org/10.1016/0360-1285(93)90022-7.
[17] P. Hernowo, C.B. Rasrendra, A. Irawan, S. Marno, Y. Meliana, O. Muraza, Y. Bindar, Volatile State Mathematical Models for Predicting Components in Biomass Pyrolysis Products, J. Eng. Technol. Sci. 54 (2022) 15878. In press, ⟨http://journals.itb.ac.id/index.php/jets/15878⟩.
[18] C. Di Blasi, C. Branca, Kinetics of primary product formation from wood pyrolysis, Ind. Eng. Chem. Res. 40 (2001) 5547–5556, https://doi.org/10.1021/ie000997e.
[19] M.G. Grønli, G. Varhegyi, C. Di Blasi, Thermogravimetric analysis and devolatilization kinetics of wood, Ind. Eng. Chem. Res. 41 (2002) 4201–4208, https://doi.org/10.1021/ie0201157.
[20] C. Di Blasi, G. Signorelli, C.D. Russo, G. Rea, Product distribution from pyrolysis of wood and agricultural residues, Ind. Eng. Chem. Res. 38 (1999) 2216–2224, https://doi.org/10.1021/ie980711u.
[21] C. Branca, C. Di Blasi, A. Galgano, Chemical characterization of volatile products of biomass pyrolysis under significant reaction-induced overheating, J. Anal. Appl. Pyrolysis. 119 (2016) 8–17, https://doi.org/10.1016/j.jaap.2016.04.004.
[22] C. Branca, C. Di Blasi, C. Mango, I. Hrablay, Products and kinetics of glucomannan pyrolysis, Ind. Eng. Chem. Res. 52 (2013) 5030–5039, https://doi.org/10.1021/ie400155x.
[23] D. Neves, H. Thunman, A. Matos, L. Tarelho, A. Gómez-Barea, Characterization and prediction of biomass pyrolysis products, Prog. Energy Combust. Sci. 37 (2011) 611–630, https://doi.org/10.1016/j.pecs.2011.01.001.
[24] E. Ranzi, A. Cuoci, T. Faravelli, A. Frassoldati, G. Migliavacca, S. Pierucci, S. Sommariva, Chemical kinetics of biomass pyrolysis, Energy and Fuels 22 (2008) 4292–4300, https://doi.org/10.1021/ef800551t.
[25] C.Di Blasi, Modeling chemical and physical processes of wood and biomass pyrolysis, Prog. Energy Combust. Sci. 34 (2008) 47–90, https://doi.org/10.1016/j.pecs.2006.12.001.
[26] M.J. Prins, K.J. Ptasinski, F.J.J.G. Janssen, Torrefaction of wood part 1: weight loss kinetics, J. Anal. Appl. Pyrolysis. 77 (2006) 28–34, https://doi.org/10.1016/j.jaap.2006.01.002.
[27] F. Shafizadeh, Pyrolytic reactions and products of biomass, in: R.P. Overend, T. A. Milne, L.K. Mudge (Eds.), Fundamentals of Thermochemical Biomass Conversion, Springer, 1985, pp. 183–217.
[28] M.J. Antal, Biomass pyrolysis: A review of the literature part 2 - lignocellulose pyrolysis, Adv. Sol. Energy (1985) 175–255, https://doi.org/10.1007/978-1-4613-9951-3_4.
[29] D.B. Anthony, J.B. Howard, Coal devolatilization and hydrogasification, AIChE J. 22 (1976) 625–656.
[30] E.M. Suuberg, W.A. Peters, J.B. Howard, Product composition and kinetics of lignite pyrolysis, Ind. Eng. Chem. Process Des. Dev. 17 (1978) 37–46, https://doi.org/10.1021/i260065a008.
[31] T.R. Nunn , Rapid Pyrolysis of Sweet Gum Wood and Milled Wood Lignin, 1981.
[32] K. Miura, A new and simple method to estimate f(E) and k0(E) in the distributed activation energy model from three sets of experimental data, Energy Fuels 9 (1995) 302–307, https://doi.org/10.1021/ef00050a014.
[33] J. Cai, W. Wu, R. Liu, An overview of distributed activation energy model and its application in the pyrolysis of lignocellulosic biomass, Renew. Sustain. Energy Rev. 36 (2014) 236–246, https://doi.org/10.1016/j.rser.2014.04.052.
[34] F. Shafizadeh, Introduction to pyrolysis of biomass, J. Anal. Appl. Pyrolysis. 3 (1982) 283–305, https://doi.org/10.1016/0165-2370(82)80017-X.
[35] C.A. Zaror, D.L. Pyle, The pyrolysis of biomass: A general review, Proc. Indian Acad. Sci. Sect. C Eng. Sci. 5 (1982) 269–285.
[36] R. Font, A. Marcilla, E. Verdu, J. Devesa, Kinetics of the pyrolysis of almond shells and almond shells impregnated with CoCl2 in a fluidized bed reactor and in a pyroprobe 100, Ind. Eng. Chem. Res. 29 (1990) 1846–1855, https://doi.org/10.1021/ie00105a016.
[37] C.J. Mill, Pyrolysis of Fine Coal Particles at High Heating Rate and Pressure, 2000.
[38] Y. Bindar, New correlations for coal and biomass pyrolysis performances with coal-biomass type number and temperature, J. Eng. Technol. Sci. 45 (2013) 275–293.
[39] T.R. Nunn, J.B. Howard, J.P. Longwell, W.A. Peters, Product compositions and kinetics in the rapid pyrolysis of sweet gum hardwood, Ind. Eng. Chem. Process Des. Dev. 24 (1985) 836–844, https://doi.org/10.1021/i200030a053.
[40] C. Branca, P. Giudicianni, C. Di Blasi, GC/MS characterization of liquids generated from low-temperature pyrolysis of wood, Ind. Eng. Chem. Res. 42 (2003) 3190–3202, https://doi.org/10.1021/ie030066d.
[41] S. Niksa, Predicting the rapid devolatilization of diverse forms of biomass with bio-flashchain, Proc. Combust. Inst. 28 (2000) 2727–2733, https://doi.org/10.1016/S0082-0784(00)80693-1.
[42] W.C. Xu, A. Tomita, Effect of coal type on the flash pyrolysis of various coals, Fuel 66 (1987) 627–631, https://doi.org/10.1016/0016-2361(87)90270-5.
[43] A. Sharma, V. Pareek, D. Zhang, Biomass pyrolysis – a review of modelling, process parameters, and catalytic studies, Renew. Sustain. Energy Rev. 50 (2015) 1081–1096, https://doi.org/10.1016/j.rser.2015.04.193.
[44] W.C. Park, A. Atreya, H.R. Baum, Experimental and theoretical investigation of heat and mass transfer processes during wood pyrolysis, Combust. Flame. 157 (2010) 481–494, https://doi.org/10.1016/j.combustflame.2009.10.006.
[45] E. Suhendi, T. Kurniawan, A.Y. Pradana, V.Z. Giffari, The effect of time on the activation of bayah natural zeolite for use in palm oil shell pyrolysis, Bull. Chem. React. Eng. Catal. 16 (2021) 588–600, https://doi.org/10.9767/bcrec.16.3.10313.588-600.
[46] Y. Huang, Y. Gao, H. Zhou, H. Sun, J. Zhou, S. Zhang, Pyrolysis of palm kernel shell with internal recycling of heavy oil, Bioresour. Technol. 272 (2019) 77–82, https://doi.org/10.1016/j.biortech.2018.10.006.

[47] S.J. Kim, S.H. Jung, J.S. Kim, Fast pyrolysis of palm kernel shells: influence of operation parameters on the bio-oil yield and the yield of phenol and phenolic compounds, Bioresour. Technol. 101 (2010) 9294–9300, https://doi.org/10.1016/j.biortech.2010.06.110.
[48] K.H. Khor, K.O. Lim, Z.A. Zainal, Characterization of bio-oil: A by-product from slow pyrolysis of oil palm empty fruit bunches, Am. J. Appl. Sci. 6 (2009) 1647–1652, https://doi.org/10.3844/ajassp.2009.1647.1652.
[49] A.E. Putun, A. Ozcan, E. Putun, Pyrolysis of hazelnut shells in a fixed-bed tubular reactor: yields and structural analysis of bio-oil, J. Anal. Appl. Pyrolysis. 52 (1999) 33–49, https://doi.org/10.1016/S0165-2370(99)00044-3.
[50] A. Demirbas, The influence of temperature on the yields of compounds existing in bio-oils obtained from biomass samples via pyrolysis, Fuel Process. Technol. 88 (2007) 591–597, https://doi.org/10.1016/j.fuproc.2007.01.010.
[51] Z. Wang, J. Cao, J. Wang, Pyrolytic characteristics of pine wood in a slowly heating and gas sweeping fixed-bed reactor, J. Anal. Appl. Pyrolysis. 84 (2009) 179–184, https://doi.org/10.1016/j.jaap.2009.02.001.
[52] K. Smets, S. Schreurs, R. Carleer, J. Yperman, Valorization of raspberry seed cake by flash and slow pyrolysis: Product yield and characterization of the liquid and solid fraction, J. Anal. Appl. Pyrolysis. 107 (2914) 289–297. doi:⟨https://doi.org/10.1016/j.jaap.2014.03.014⟩.
[53] S. Yorgun, D. Yıldız, Slow pyrolysis of paulownia wood: effects of pyrolysis parameters on product yields and bio-oil characterization, J. Anal. Appl. Pyrolysis. 114 (2015) 68–78, https://doi.org/10.1016/j.jaap.2015.05.003.
[54] K.H. Khor, K.O. Lim, Slow pyrolysis of oil palm empty fruit bunches, Int. Energy J. 9 (2008) 181–188, http://www.rericjournal.ait.ac.th/index.php/reric/article/view/484.
[55] P. Ruengvilairat, H. Tanatavikorn, T. Vitidsant, Bio-oil production by pyrolysis of oil palm empty fruit bunch in nitrogen and steam atmospheres, J. Sustain. Bioenergy Syst. 2 (2012) 75–85, https://doi.org/10.4236/jsbs.2012.24011.
[56] C. Branca, Di Blas, A unified mechanism of the combustion reactions of lignocellulosic fuels, Thermochim. Acta. 565 (2013) 58–64, https://doi.org/10.1016/j.tca.2013.04.014.
[57] M.A. Aziz, K.M. Sabil, Y. Uemura, L. Ismail, A study on torrefaction of oil palm biomass, J. Appl. Sci. 12 (2012) 1130–1135, https://doi.org/10.3923/jas.2012.1130.1135.
[58] N. Sbirrazzuoli, Interpretation and physical meaning of kinetic parameters obtained from isoconversional kinetic analysis of polymers, Polymers (2020) 1–19, https://doi.org/10.3390/POLYM12061280.
[59] A. Khawam, D.R. Flanagan, Role of isoconversional methods in varying activation energies of solid-state kinetics I. Isothermal kinetic studies, Thermochim. Acta. 429 (2005) 93–102, https://doi.org/10.1016/j.tca.2004.11.030.
[60] N. Sbirrazzuoli, S. Vyazovkin, A. Mititelu, C. Sladic, L. Vincent, A study of epoxy-amine cure kinetics by combining isoconversional analysis with temperature modulated DSC and dynamic rheometry, Macromol. Chem. Phys. 204 (2003) 1815–1821, https://doi.org/10.1002/macp.200350051.
[61] N. Sbirrazzuoli, A. Mititelu-Mija, L. Vincent, C. Alzina, Isoconversional kinetic analysis of stoichiometric and off-stoichiometric epoxy-amine cures, Thermochim. Acta. 447 (2006) 167–177, https://doi.org/10.1016/j.tca.2006.06.005.
[62] G. Falco, N. Guigo, L. Vincent, N. Sbirrazzuoli, FA polymerization disruption by protic polar solvents, Polymers (2018) 1–14, https://doi.org/10.3390/polym10050529.
[63] A. Sangregorio, N. Guigo, E. de Jong, N. Sbirrazzuoli, Kinetics and chemorheological analysis of cross-linking reactions in humins, Polymers (2019) 1–15, https://doi.org/10.3390/polym11111804.
[64] A. Codou, M. Moncel, J.G. van Berkel, N. Guigo, N. Sbirrazzuoli, Glass transition dynamics and cooperativity length of poly(ethylene 2,5-furandicarboxylate) compared to poly(ethylene terephthalate), Phys. Chem. Chem. Phys. 18 (2016) 16647–16658, https://doi.org/10.1039/C6CP01227B.
[65] S. Vyazovkin, On the phenomenon of variable activation energy for condensed phase reactions, New J. Chem. 24 (2000) 913–917, https://doi.org/10.1039/b004279j.
[66] S. Vyazovkin, Kinetic concepts of thermally stimulated reactions in solids: A view from a historical perspective, Int. Rev. Phys. Chem. 19 (2000) 45–60, https://doi.org/10.1080/014423500229855.
[67] S. Vyazovkin, C.A. Wight, Kinetics in solids, Annu. Rev. Phys. Chem. 48 (1997) 125–149, https://doi.org/10.1146/annurev.physchem.48.1.125.
[68] A.K. Galwey, What is meant by the term 'variable activation energy' when applied in the kinetic analyses of solid state decompositions (crystolysis reactions)? Thermochim. Acta. 397 (2003) 249–268, https://doi.org/10.1016/S0040-6031(02)00271-X.
[69] S. Vyazovkin, Reply to "what is meant by the term 'variable activation energy' when applied in the kinetics analyses of solid state decompositions (crystolysis reactions)? Thermochim. Acta 397 (2003) 269–271, https://doi.org/10.1016/S0040-6031(02)00391-X.
[70] C.N. Hinshelwood, The kinetics of chemical change in gaseous systems, 1926.
[71] E.A. Moelwyn-Hughes, The chemical statics and kinetics of solutions (Physical chemistry), 1971.
[72] S. Vyazovkin, Two types of uncertainty in the values of activation energy, J. Therm. Anal. Calorim. 64 (2001) 829–835, https://doi.org/10.1023/A:1011573218107.
[73] W. de Jong, A. Pirone, M.A. Wojtowicz, Pyrolysis of miscanthus giganteus and wood pellets: TG-FTIR analysis and reaction kinetics, Fuel 82 (2003) 1139–1147, https://doi.org/10.1016/S0016-2361(02)00419-2.

CHEMICAL COMPONENT YIELD 2022

ORIGINALITY REPORT

16%	12%	10%	4%
SIMILARITY INDEX	INTERNET SOURCES	PUBLICATIONS	STUDENT PAPERS

PRIMARY SOURCES

1	pubag.nal.usda.gov Internet Source	1%
2	espace2.etsmtl.ca Internet Source	1%
3	Pandit Hernowo, Soen Steven, Elvi Restiawaty, Yazid Bindar. "Nature of mathematical model in lignocellulosic biomass pyrolysis process kinetic using volatile state approach", Journal of the Taiwan Institute of Chemical Engineers, 2022 Publication	1%
4	journals.itb.ac.id Internet Source	1%
5	Yongyu Ding, Jiacheng Liu, Wen Qiu, Qunpeng Cheng, Guozhi Fan, Guangsen Song, Shunxi Zhang. "Knetics and behavior analysis of lobster shell pyrolysis by TG-FTIR and Py-GC/MS", Journal of Analytical and Applied Pyrolysis, 2022 Publication	1%

6	link.springer.com Internet Source	1 %
7	www.tandfonline.com Internet Source	1 %
8	addi.ehu.es Internet Source	<1 %
9	www.mdpi.com Internet Source	<1 %
10	Submitted to Universiti Brunei Darussalam Student Paper	<1 %
11	SFPE Handbook of Fire Protection Engineering, 2016. Publication	<1 %
12	ebuah.uah.es Internet Source	<1 %
13	L. Buján, P. Fernández, N. Lafuente, M. Aldonza, A. M. Bermejo. "COMPARISON OF TWO CHROMATOGRAPHIC METHODS FOR THE DETERMINATION OF COCAINE AND ITS METABOLITES IN BLOOD AND URINE", Analytical Letters, 2007 Publication	<1 %
14	www.researchgate.net Internet Source	<1 %

15	Banshidhar Majhi, Hasan Shalabi ., Mowafak Fathi ., Abbas M. Ali .. "Detection of Parallelism in Sequential Programs Based on Functional Partitioning", Information Technology Journal, 2005 Publication	<1 %
16	repository.nwu.ac.za Internet Source	<1 %
17	Soen Steven, Elvi Restiawaty, Pasymi Pasymi, Yazid Bindar. "Three-dimensional flow modelling of air and particle in a low-density biomass combustor chamber at various declination angles of tangential and secondary air pipes", Powder Technology, 2022 Publication	<1 %
18	Soen Steven, Elvi Restiawaty, Yazid Bindar. "Routes for energy and bio-silica production from rice husk: A comprehensive review and emerging prospect", Renewable and Sustainable Energy Reviews, 2021 Publication	<1 %
19	archive.org Internet Source	<1 %
20	Sukarni Sukarni. "Thermogravimetric analysis of the combustion of marine microalgae	<1 %

	Spirulina platensis and its blend with synthetic waste", Heliyon, 2020 Publication	
21	mostwiedzy.pl Internet Source	<1 %
22	daneshyari.com Internet Source	<1 %
23	journals.plos.org Internet Source	<1 %
24	jptcp.com Internet Source	<1 %
25	Submitted to Universidad Estadual Paulista Student Paper	<1 %
26	amb-express.springeropen.com Internet Source	<1 %
27	www.freepatentsonline.com Internet Source	<1 %
28	Elvi Restiawaty, Yazid Bindar, Khariful Syukri, Oky Syahroni, Soen Steven, Ria Ayu Pramudita, Yogi Wibisono Budhi. "Production of acid-treated-biochar and its application to remediate low concentrations of Al(III) and Ni(II) ions in the water contaminated with red mud", Biomass Conversion and Biorefinery, 2022 Publication	<1 %

29	Yao, Dingding, Qiang Hu, Daqian Wang, Haiping Yang, Chunfei Wu, Xianhua Wang, and Hanping Chen. "Hydrogen production from biomass gasification using biochar as a catalyst/support", Bioresource Technology, 2016. Publication	<1 %
30	academic.oup.com Internet Source	<1 %
31	www.hindawi.com Internet Source	<1 %
32	Submitted to Unviersidad de Granada Student Paper	<1 %
33	ejournal.undip.ac.id Internet Source	<1 %
34	pure.tue.nl Internet Source	<1 %
35	"Coal and Biomass Gasification", Springer Science and Business Media LLC, 2018 Publication	<1 %
36	Yongyu Ding, Jiacheng Liu, Wen Qiu, Qunpeng Cheng, Guozhi Fan, Guangsen Song, Shunxi Zhang. "Kinetics and behavior analysis of lobster shell pyrolysis by TG-FTIR and Py-GC/MS", Journal of Analytical and Applied Pyrolysis, 2022 Publication	<1 %

37	backend.orbit.dtu.dk Internet Source	<1 %
38	dmbj.org.rs Internet Source	<1 %
39	dspace.pondiuni.edu.in Internet Source	<1 %
40	epdf.pub Internet Source	<1 %
41	livrepository.liverpool.ac.uk Internet Source	<1 %
42	mdpi-res.com Internet Source	<1 %
43	onlinelibrary.wiley.com Internet Source	<1 %
44	ris.utwente.nl Internet Source	<1 %
45	Bingan Xu, Peter Smith. "Dehydration kinetics of boehmite in the temperature range 723–873K", Thermochimica Acta, 2012 Publication	<1 %
46	J. R. GIBBINS, C. K. MAN, K. J. PENDLEBURY. "Determination of Rapid Heating Volatile Matter Contents as a Routine Test", Combustion Science and Technology, 1993 Publication	<1 %

47	Jinsi Li, Xuerong Fang, Xin Ming. "Visibly Emitting Thiazolyl-Uridine Analogues as Promising Fluorescent Probes", The Journal of Organic Chemistry, 2020 Publication	<1 %
48	K.H. Khor, K.O. Lim, Z.A. Zainal. "Characterization of Bio-Oil: A By-Product from Slow Pyrolysis of Oil Palm Empty Fruit Bunches", American Journal of Applied Sciences, 2009 Publication	<1 %
49	Khawam, A.. "Role of isoconversional methods in varying activation energies of solid-state kinetics", Thermochimica Acta, 20050501 Publication	<1 %
50	Zabaniotou, A.. "Evaluation of utilization of corn stalks for energy and carbon material production by using rapid pyrolysis at high temperature", Fuel, 200805 Publication	<1 %
51	coek.info Internet Source	<1 %
52	core.ac.uk Internet Source	<1 %
53	d-nb.info Internet Source	<1 %

54	docplayer.org Internet Source	<1 %
55	etd.auburn.edu Internet Source	<1 %
56	open.library.ubc.ca Internet Source	<1 %
57	tel.archives-ouvertes.fr Internet Source	<1 %
58	www.cawq.ca Internet Source	<1 %
59	zero.sci-hub.se Internet Source	<1 %
60	Wang, Z.. "Pyrolytic characteristics of pine wood in a slowly heating and gas sweeping fixed-bed reactor", Journal of Analytical and Applied Pyrolysis, 200903 Publication	<1 %
61	"Progress in Thermochemical Biomass Conversion", Wiley, 2001 Publication	<1 %
62	Jakub Mularski, Norbert Modliński. "Entrained flow coal gasification process simulation with the emphasis on empirical devolatilization models optimization procedure", Applied Thermal Engineering, 2020 Publication	<1 %

63 Mohammad Hosseini Rahdar, Fuzhan Nasiri, Bruno Lee. "A Review of Numerical Modeling and Experimental Analysis of Combustion in Moving Grate Biomass Combustors", Energy & Fuels, 2019 <1%
Publication

Exclude quotes	On	Exclude matches	Off
Exclude bibliography	On		

CHEMICAL COMPONENT YIELD 2022

GRADEMARK REPORT

FINAL GRADE

/0

GENERAL COMMENTS

Instructor

PAGE 1

PAGE 2

PAGE 3

PAGE 4

PAGE 5

PAGE 6

PAGE 7

PAGE 8

PAGE 9

PAGE 10

PAGE 11

PAGE 12

PAGE 13

PAGE 14